Journal of ELECTRONIC MATERIALS, Vol. 49, No. 9, 2020
https://doi.org/10.1007/s11664-020-08073-2

TOPICAL COLLECTION: 18TH CONFERENCE ON DEFECTS (DRIP XVIII)

A Comparison of Defects Between InAs Single Crystals Grown by LEC and VGF Methods

GUIYING SHEN,[1,3] YOUWEN ZHAO,[1,2,3,4] JING SUN,[1,2] JINGMING LIU,[1] ZHIYUAN DONG,[1] HUI XIE,[1] FENGHUA WANG,[1] and JUN YANG[1]

1.—Key Laboratory of Semiconductor Materials Science, Beijing Key Laboratory of Low Dimensional Semiconductor Materials and Devices, Institute of Semiconductors, Chinese Academy of Sciences, P.O. Box 912, Beijing 100083, China. 2.—College of Materials Science and Opto-electronic Technology, University of Chinese Academy of Sciences, Beijing 100049, China. 3.—Zhuhai DT Wafer-tech Co., LTD, South Jinrui No. 2 Road, Jingding Hi-Tech Industrial Development Zone, Zhuhai, Guangdong, China. 4.—e-mail: shenguiying@semi.ac.cn

InAs single crystals grown by the liquid-encapsulated Czochralski (LEC) method and vertical gradient freezing (VGF) are studied by low-temperature photoluminescence spectroscopy, infrared transmission and reflectance spectroscopy, double-crystal x-ray diffraction and Hall effect measurement, respectively. A properly controlled etching solution is used to reveal beautiful square dislocation etch pits in the crystals. In addition to extremely low dislocation density, the concentration of native defects in the VGF-InAs single crystals is much lower than that in LEC-InAs, giving VGF-InAs better electrical and optical properties. The nature of the defects in InAs single crystals is discussed by considering the variation in stoichiometry and environment during the crystal growth processes.

Key words: InAs single crystals, etch pits, native defects, LEC, VGF

INTRODUCTION

Indium arsenide (InAs) single crystals have emerged as highly promising substrate materials among the III-V compound semiconductors for use in very high-speed (and lower power) electronics and mid-infrared optoelectronics,[1,2] due to their relatively narrow band gap of 0.36 eV. Moreover, InAs, with a lattice constant of 0.606 nm, is a suitable substrate for the growth of InAsSb/InAsPSb, an InNAsSb heterojunction, which is critical for the preparation of infrared light-emitting devices with wavelengths of 2–14 μm.[3–6]

A large percentage of commercial bulk InAs single crystal is grown by the liquid-encapsulated Czochralski (LEC)[7] method. With this method, a glass material, mainly boron oxide for InAs, is used to encapsulate the melt. Although InAs single crystals of good quality can be obtained, twinning, impurity contamination and high concentrations of dislocations are the main issues with this method.[8] In order to counter this disadvantage, a vertical gradient freezing (VGF)[9] method has been developed to grow InAs single crystals with better crystalline quality. The advantage of VGF technology originates from two key features: (a) a low thermal gradient and (b) a closed growing environment. However, the crystalline quality of InAs single crystals grown by VGF has not been studied extensively.

High concentrations of purely structural defects such as dislocations, impurities and vacancies are easily formed in the process of crystal growth.[10–12] The presence of these defects in InAs substrates, which may propagate into epitaxy layers grown thereon, is potentially detrimental to device

(Received November 7, 2019; accepted March 11, 2020; published online March 28, 2020)

performance. Various crystal defects will be formed using LEC and VGF techniques, which have different crystal growth conditions. In this work, a proper method is used to directly observe the chemical etch pits which exhibit crystal defects. Together with the electrical and optical properties, a comparison of native defects in LEC-InAs and VGF-InAs is systematically investigated.

EXPERIMENTAL

Un-doped InAs ingots were grown at the authors' laboratory by LEC and VGF methods with boron oxide as an encapsulation. A quartz crucible was used in the LEC technique, while a boron nitride crucible sealed in a quartz tube was used in VGF. Wafers with (100)-orientation sliced from these ingots were used as samples for the experiment, and were subjected to chemical–mechanical polishing to obtain a mirror-like surface. The epi-ready InAs samples were finally obtained through a multi-step cleaning process.

In order to study the behavior of native defects, the electrical and optical properties of LEC-InAs and VGF-InAs were determined by Hall measurement, infrared reflectance spectroscopy, and low-temperature photoluminescence (PL), respectively. The samples were then corroded in an optimized etchant[13] to clearly display the dislocation etch pits on InAs wafers grown by different methods. After the corrosion, an optical microscope with a maximum magnification of 1000× was used to observe the etching profile. A 37-point etch pit density (EPD) map was used to determine the dislocation density of the LEC-InAs and VGF-InAs.[14]

RESULTS AND DISCUSSION

Characterization of Crystal Quality

Figure 1 shows the typical etch pits on the surface of (100) LEC-InAs and VGF-InAs developed by an etchant. It is revealed that tetragonal pyramid pits (D-pits) with their long axis aligned parallel to the $<1\bar{1}0>$ direction are formed on LEC-InAs surfaces. However, etch pits developed on VGF-InAs surfaces can be classified into dislocation pits (D-pits) and shallow or saucer pits (S-pits), which are similar to etch pits revealed on GaAs and GaP.[15,16] The identification of the pits is quite straightforward: D-pits have an apex or point, while S-pits are shallow, round and flat-bottomed. Compared with LEC-InAs, the EPD of VGF-InAs is less than $\sim 500\ cm^{-2}$, while the average EPD of LEC-InAs is as high as about $10^4\ cm^{-2}$. In addition, the density of S-pits in InAs wafers grown by VGF is $\sim 400\ cm^{-2}$, while LEC-grown InAs shows either no S-pits or a several-orders-of-magnitude reduction of the S-pits density. Since both LEC- and the VGF-InAs were grown without doping, the high density of S-pits in VGF-InAs is not directly related to impurities. Researchers have conducted many experiments and have attributed the nature of the S-pits to point defects,[17] mixed dislocations and etching vacancy aggregates.[18] Further studies are needed for confirmation.

A high density of dislocations in LEC-InAs single crystals indicates poor crystallization quality due to the high thermal gradients in the LEC method, which allow dislocation motion by climb. In order to evaluate the crystal quality of LEC-InAs and VGF-InAs, the typical double-crystal x-ray diffraction (DCXRD) curves are plotted in Fig. 2 The InAs sample grown by the LEC technique shows that the full width at half maximum (FWHM) of (004) reflection is 20 arcsec, which is obviously broader than FWHM = 14 arcsec of the VGF-InAs sample. Thus, it is revealed that VGF-InAs single crystals with low EPD possess good structural quality and excellent composition uniformity. There are two possible reasons for this phenomenon: (a) extremely low temperature gradient with the VGF technique, and (b) the formation of the VGF-InAs single crystal inside the sealed quartz tube using a boron nitride crucible, which avoids the issues of contaminants.

Native Defects

The Hall measurement is used to study the carrier concentration which is determined by residual impurities and native defects generated both

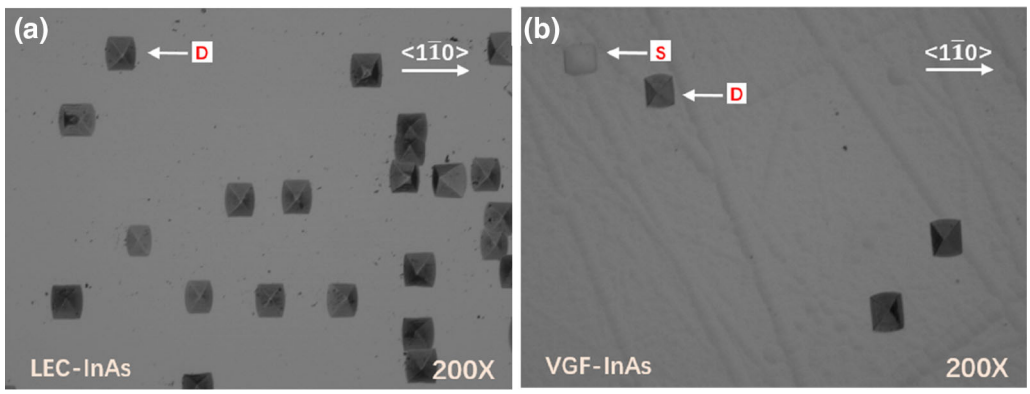

Fig. 1. Dislocation etch pits on (a) LEC-InAs and (b) VGF-InAs surfaces.

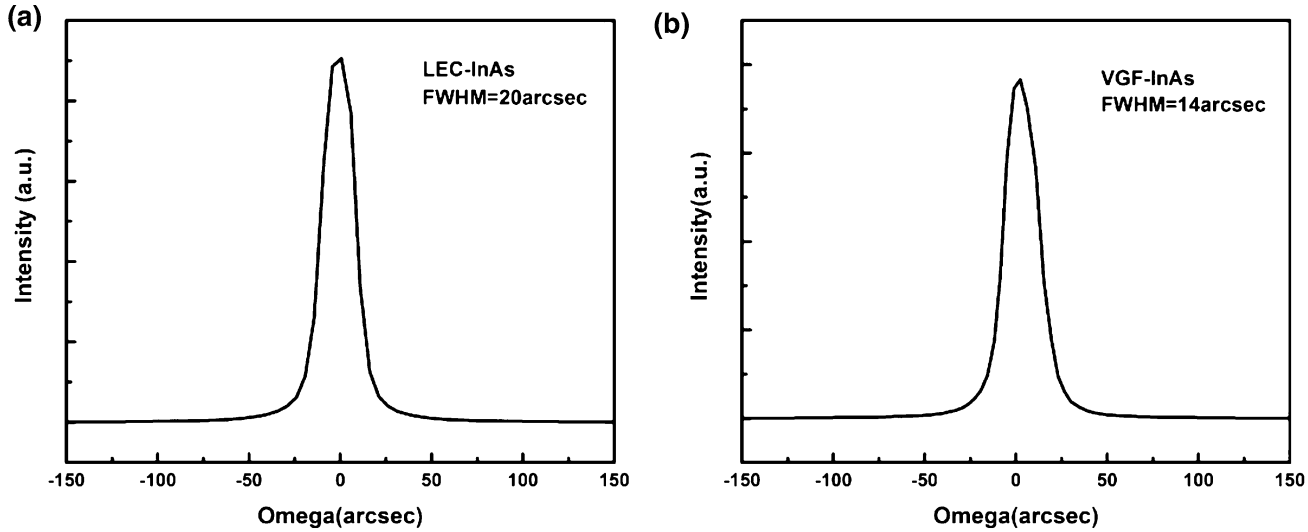

Fig. 2. Double-crystal x-ray diffraction curves for (a) LEC-InAs and (b) VGF-InAs single crystals.

Table I. Electrical properties of InAs single crystals grown by LEC and VGF methods

Growth method	Mobility (10^4 cm^2/V s)	Carrier concentration (10^{16} cm^{-3})
LEC	1.99–2.50	1.97–6.63
VGF	2.43–2.59	1.72–2.16

during the process of crystal growth and also during the cooling process after crystal growth. Table I shows the values of the mobility and carrier concentration of InAs single crystals grown by the LEC and VGF methods. Un-doped InAs single crystals grown by the LEC and VGF methods are both found to be of an n-type, with a free-electron concentration of $\sim 10^{16}$ cm^{-3}, and it is concluded that the background donors are related to native defects rather than chemical impurities.[12] Compared with LEC-InAs, VGF-InAs has higher mobility and lower carrier concentration, indicating better electrical purity. Since a large amount of arsenic (As) volatilizes in the process of crystal growth by LEC, a high concentration of donor-like As vacancy defects can be easily formed in the In-rich condition, which results in the increased carrier concentration in LEC-InAs. Moreover, carbon contamination from the heater and insulation cover made of graphite can also be incorporated into InAs single crystals. Hence, it is expected that a higher concentration of point defects and C atom-related defects exists in LEC-InAs single crystals. However, InAs single crystals grown by VGF are formed inside the sealed quartz tube, and hence there are no contaminant issues. Also, the crystal must be of good stoichiometry. Thus, it is expected that VGF-InAs performs better with regard to native defects and electrical properties.

It is very difficult to obtain details about defect levels using measurement by deep-level transient spectroscopy (DLTS) due to the extremely narrow band gap of InAs. Therefore, low-temperature infrared photoluminescence (PL) was used to qualitatively study the native defects in InAs using a Bruker Vertex 80v with a sufficiently high signal-to-noise ratio (SNR). A semiconductor laser operating at 639 nm with typical power of 50 mW was used as the excitation source.[19] The PL intensity distribution of LEC-InAs and VGF-InAs at 10 K is shown in Fig. 3 as a function of energy. As shown in the PL spectra of the LEC-InAs single crystal, five distinct PL peaks labeled A, B, C, D and E are clearly resolved. Peak A located at 415 meV corresponds to electron–hole recombination emission,[20] which corresponds to the calculated value of energy gap at 10 K, according to the Varshni equation[20]:

$$E_g(T) = E_{g0} - \alpha T^2/(T+\beta) \quad (T \geq 10\,\mathrm{K}), \qquad (1)$$

where $E_{g0} = 415$ meV, $\alpha = 0.276$ meV/K, and $\beta = 83$ K for InAs. Peaks B and C located at 412 meV and 403 meV are attributed to an emission process involving either shallow impurities or defects[21] whose binding energy is about 3 meV and 12 meV, respectively. Peak D at about 383 meV is assigned to CH_3, which is a type of acceptor defect with ionization of 32 meV.[22] The

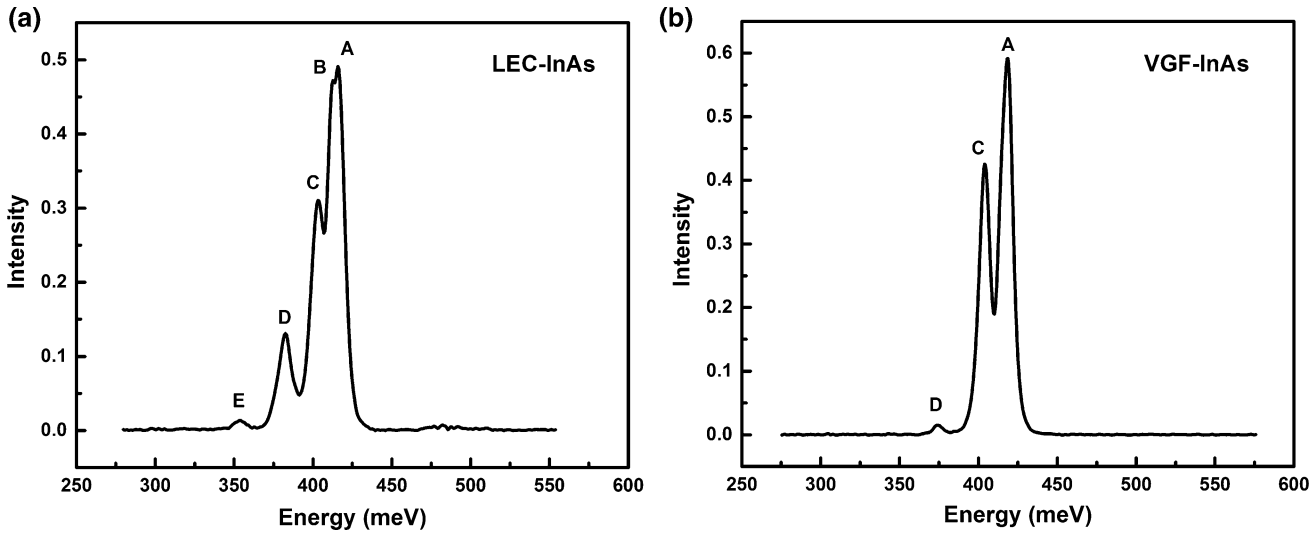

Fig. 3. PL spectra of (a) LEC-InAs and (b) VGF-InAs single crystals measured at 10 K.

weak peak E located at 353 meV is a phonon replica of peak D. For the PL spectrum of the VGF-InAs sample, the dominant peak A shifts from 415 meV to 418 meV, which is very close to the reported 4.2 K band-gap value. This peak shift is believed to be due to the relatively high crystal quality of VGF-InAs single crystals, which also have high electrical purity. In addition, peak B, which is related to an extremely shallow level, disappears in the PL spectrum of VGF-InAs due to the annihilation of the related native defect. The intensity of peak D decreases significantly and its phonon replica disappears, which indicates that there is a lower concentration of indium-related vacancy defects in VGF-InAs than in LEC-InAs.

Since native defects such as vacancies, antisites and other complex defects inevitably exist in InAs single crystals, the optical absorption for below-band-gap energy photons has been found to be crucial for characterizing these defects. In order to study the role of these defects and the relation between defect and growth method, transmission spectra of LEC-InAs and VGF-InAs were measured at room temperature using an FTS-60v Fourier transform infrared (FTIR) spectrometer system, as shown in Fig. 4. For VGF-InAs single crystals, the transmission remains almost constant at a relatively high value of nearly 50% from 500 cm^{-1} to 2500 cm^{-1}, while it decreases rapidly to almost zero with wavenumbers exceeding 2500 cm^{-1}, which corresponds to the band-to-band absorption. However, the transmission of LEC-InAs single crystals changes markedly especially when the wavenumber is less than 1100 cm^{-1}. Combined with the experimental results above, the absorption related to the native defects may be responsible for the low transmission in the wavenumber range of 500–1500 cm^{-1}. In the case of the VGF-InAs sample, the flat transmission curve is indicative of the relatively

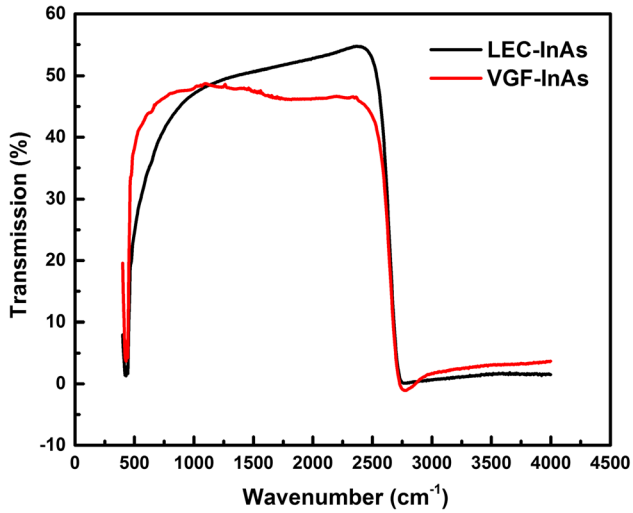

Fig. 4. Transmission spectra of LEC-InAs (dark line) and VGF-InAs (red line) single crystals measured at 300 K (Color figure online).

low concentration of native defects compared with that of LEC-InAs. Hence, VGF-InAs single crystals with better structure and composition uniformity have more homogeneous infrared absorption characteristics.

In order to study the defect absorption of InAs, a reflectance spectrum was obtained using a Bruker Vertex 80v with a normal incident beam, which is shown in Fig. 5. The inset depicts the theoretical value of R as a function of wavenumber. From classical dispersion theory, for 3 $\mu m < \lambda < 8$ μm (which is in the wavenumber range of 1300–2800 cm^{-1}), the refractive index can be described as[23]:

$$n = \left[11.1 + \frac{0.71}{1 - 6.5 \times \lambda^{-2}} + \frac{2.75}{1 - 2085 \times \lambda^{-2}} - 6 \times 10^{-4} \times \lambda^{2}\right]^{1/2} \quad (2)$$

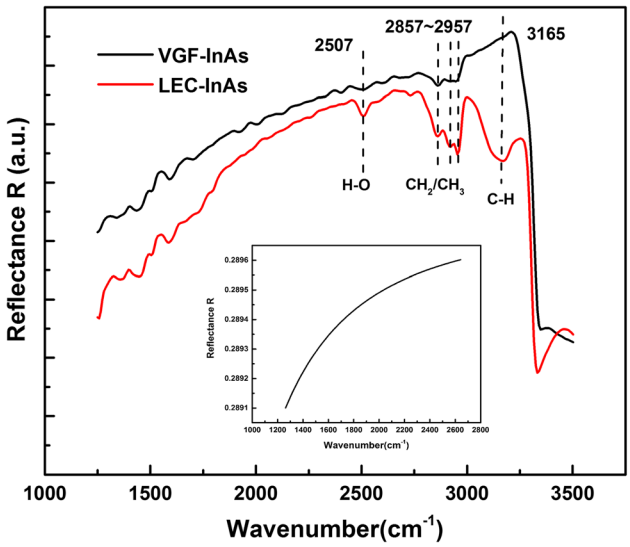

Fig. 5. Relative reflectance R of LEC-InAs and VGF-InAs as a function of wavenumber. The inset displays the results of absolute reflectance of InAs by theoretical calculation.

where λ is the wavelength in μm at 300 K. In theory, reflectivity R for a normally incident beam can be calculated from the refractive index of InAs using the following expression[24]:

$$R = \left(\frac{n-1}{n+1}\right)^2. \quad (3)$$

Hence, the theoretical value of reflectance R, which ignores the effect of crystal defects in InAs, can be obtained as shown in the inset in Fig. 5. For InAs single crystals with a perfect crystal structure, the reflectance increases slowly from 1300 cm^{-1} to 2800 cm^{-1} due to the slight increase in the refractive index with the wavenumber.

Compared with the calculated results, the reflectance R of LEC-InAs and VGF-InAs shows an increasing trend as well, whereas it decreases markedly at wavenumbers exceeding about 3340 cm^{-1} corresponding to a band-to-band absorption edge, which is in agreement with the interpretation of peak A in the PL spectra. In addition, some absorption peaks with high frequencies downward appear in the reflectance curves of LEC-InAs and VGF-InAs single crystals, which correspond to local vibration mode (LVM)-related absorption of light impurities. The reflectance curve of LEC-InAs presents three groups of typical LVM peaks at 2507 cm^{-1}, 2857–2957 cm^{-1} and 3165 cm^{-1}, which can be easily assigned to the stretching vibration modes of H-O, CH_2/CH_3 and C-H complex defects, respectively,[25,26] while for VGF-InAs single crystals, the LVM peak located at 3165 cm^{-1} disappears, which demonstrates that no C-H complex defects appear in VGF-InAs single crystals. In addition, the intensity of other peaks related to H-O and CH_2/CH_3 obviously decreases, which indicates that a low concentration of defects exist in VGF-InAs. Hence, it can be concluded that C, H and O atoms are the main impurities, and the related defects H-O, CH_2/CH_3 and C-H, acting as extrinsic defects, are inevitably formed in the process of both LEC and VGF growth. We have discussed the structure configuration, electrical properties and thermal stability of these defects in detail previously.[27]

Compared with the LEC method, VGF crystal growth is carried out inside a sealed boron nitride crucible, which avoids the contamination of C atoms from the graphite heater and insulation cover used in the LEC process. Additionally, the temperature gradient of VGF is extremely small, which directly results in a low average EPD in VGF-InAs. Hence, VGF-InAs with a low number of structural defects must be of high crystal quality and electrical purity, which is demonstrated well in DCXRD curves and Hall measurements, while in the case of the LEC method, stoichiometry is not easily maintained due to the dissociation of arsenic, which is easily volatile. Also, the native defects related to C, H and O impurities can be easily doped during growth in LEC-InAs single crystals due to the high concentration. The same conclusion can be obtained with regard to the PL, transmission and reflectance spectra of LEC-InAs and VGF-InAs. The disappearance of peak B in Fig. 3b may be attributed to the absence of C-H complex defects in VGF-InAs, which have no issues of contamination by the graphitic heater and insulation cover. Similarly, the concentration of CH_3-related native defects in VGF-InAs represented by peak D is decreased due to the sealed environment for single-crystal growth.

CONCLUSION

In summary, a comparison of defects between InAs single crystals grown by LEC and VGF methods has been investigated in this work. VGF-InAs single crystals have many fewer native defects and superior lattice perfection compared with LEC-InAs. Thus, VGF-InAs with better structural, electrical and optical properties represent promising materials for use in the field of high-speed electronics and mid-infrared devices.

ACKNOWLEDGMENTS

The authors gratefully acknowledge the support of the National Natural Science Foundation of China (Grant No. 61904175). We acknowledge Chen Xiren at Shanghai Institute of Technical Physics (CAS) for skillful PL measurement of our samples. We acknowledge Wang Nanlin and Wang Zixiao at Peking University for skillful infrared reflectance measurement of our samples.

REFERENCES

1. H. Lotfi, L. Li, L. Lei, H. Ye, S.M. Shazzad Rassel, Y. Jiang, R. Yang, T. Mishima, M. Santos, and J. Gupta, *Appl. Phys. Lett.* 108, 201101 (2016).

2. L. Li, Y. Jiang, H. Ye, R.Q. Yang, T.D. Mishima, M.B. Santos, and M.B. Johnson, *Appl. Phys. Lett.* 106, 251102 (2015).
3. Y.Z. Gao, X.Y. Gong, Y.S. Gui, T. Yamaguchi, and N. Dai, *Jpn. J. Appl. Phys.* 43, 1051 (2004).
4. X.Y. Gong, H. Kan, T. Makino, T. Iida, K. Watanabe, Y.Z. Gao, M. Aoyama, N.L. Rowell, and T. Yamaguchi, *Jpn. J. Appl. Phys.* 39, 5039 (2000).
5. Y.Z. Gao, T. Yamaguchi, X.Y. Gong, H. Kan, M. Aoyama, and N. Dai, *Jpn. J. Appl. Phys.* 42, 4203 (2003).
6. N.L. Rowell, T. Yamaguchi, X.Y. Gong, and H. Kan, *SPIE* 3491, 288 (2003).
7. J.B. Mullin, *Handbook of Crystal Growth*, ed. by P. Rudolph (Springer, Harbin, 2015), p. 113.
8. Y. Zhao, W. Sun, M. Duan, Z. Dong, and Z. Yang, *J. Semicond.* 27, 1391 (2006).
9. L. Reijnen, R. Brunton, and I.R. Grant, *AIP Conf. Proc.* 738, 360 (2004).
10. V.N. Morozov and V.G. Chernov, *Sov. Phys. Semicond.* 14, 863 (1980).
11. V.V. Karataev, M.G. Mil'vidskii, N.S. Rytova, and V.I. Fistul, *Sov. Phys. Semicond.* 11, 1718 (1977).
12. H.A. Tahini, A. Chroneos, S.T. Murphy, U. Schwingenschlögl, and R.W. Grimes, *J. Appl. Phys.* 114, 063517 (2013).
13. J. Sun, G. Shen, H. Xie, J. Liu, D. Yu, and Y. Zhao, *J. Cryst. Growth* 526, 125237 (2019).
14. W. Liu, M.S. Young, and H. Badawi, U.S. Patent No. US 8,361,225 B2 (2013).
15. T. Takenaka, H. Hayashi, K. Murata, and T. Inoguchi, *Jpn. J. Appl. Phys.* 17, 1145 (1978).
16. G.A. Rozgonyi and T. Lizuka, *J. Electrochem. Soc.* 120, 673 (1973).
17. G.A. Rozgonyi, A.R. Von Neida, T. Iizuka, and S.E. Haszko, *J. Appl. Phys.* 43, 3141 (1972).
18. A.G. Tweet, *J. Appl. Phys.* 30, 2002 (1959).
19. J. Shao, W. Lu, X. Lü, F. Yue, Z. Li, S. Guo, and J. Chu, *Rev. Sci. Instrum.* 77, 063104 (2006).
20. Z.M. Fang, K.Y. Ma, D.H. Jaw, R.M. Cohen, and G.B. Stringfellow, *J. Appl. Phys.* 67, 7034 (1990).
21. R.D. Grober, H.D. Drew, J.I. Chyi, S. Kalem, and H. Morkoç, *J. Appl. Phys.* 65, 4079 (1989).
22. G. Shen, Y. Zhao, Z. Dong, J. Liu, H. Xie, Y. Bai, and X. Chen, *Mater. Res. Express* 4, 036203 (2017).
23. O.G. Loimor and W.G. Spitzer, *J. Appl. Phys.* 36, 1841 (1965).
24. R. Bhat, P.S. Dutta, and S. Guha, *J. Cryst. Growth* 310, 1910 (2008).
25. J. Edward, G. Brame, and G. Jeanette, *Infrared and Raman Spectroscopy*, Vol. 1 (New York: Marcel Dekker, 1977).
26. H.A. Szymanski, *IR Theory and Practice of Infrared Spectroscopy* (New York: Plenum Press, 1964).
27. G. Shen, Y. Zhao, J. Liu, Y. Bai, Z. Dong, H. Xie, X. Chen, and J. Electronic, *Mater* 47, 4998 (2018).